Title
Vertical graphene base transistor

Journal
IEEE Electron Device Letters, 33(5)

ISSN
0741-3106

Authors
Mehr, W
Dabrowski, J
Scheytt, JC
et al.

Publication Date
2012-05-01

DOI
10.1109/LED.2012.2189193

Peer reviewed

Vertical Graphene Base Transistor

Wolfgang Mehr, Jarek Dabrowski, J. Christoph Scheytt, *Member, IEEE*, Gunther Lippert, Ya-Hong Xie, *Senior Member, IEEE*, Max C. Lemme, *Senior Member, IEEE*, Mikael Ostling, *Fellow, IEEE*, and Grzegorz Lupina

***Abstract*—We present a novel graphene-based-device concept for a high-frequency operation: a hot-electron graphene base transistor (GBT). Simulations show that GBTs have high current on/off ratios and high current gain. Simulations and small-signal models indicate that it potentially allows terahertz operation. Based on energy-band considerations, we propose a specific material solution that is compatible with SiGe process lines.**

***Index Terms*—Graphene, hot-electron transistor (HET), radio frequency (RF).**

I. Introduction

CARBON-BASED materials may enhance the performance of digital and radio frequency (RF) electronics [1]. Extensive research has been devoted to exploit the exceptional properties of graphene in field-effect transistors with a graphene channel (GFETs) [2], [3]. This has resulted in RF GFETs with transition frequencies (f_T) of several hundred gigahertz [4], [5], ambipolar RF mixers [6], and frequency multipliers [7]. However, GFETs are not suitable for logic applications due to the absence of a bandgap, and the lack of a pronounced drain-current saturation limits their potential for conventional RF amplifying circuits [8], [9].

We propose an alternative application of graphene as an extremely thin and highly conductive electrode for a hot-electron transistor (HET) with a graphene base. This graphene base transistor (GBT) combines the concept of HETs [10]–[12] with the unique properties of graphene to result in a high-frequency (HF) device that offers low off currents (I_{off}), drain-current saturation, and power amplification.

II. GBT Concept

Fig. 1(a) and (b) illustrates the difference between the GFET and the GBT. Charge carriers traverse the graphene in the GFET laterally. The GBT is based on a vertical arrangement of emitter (E), base (B), and collector (C), just like a HET or a vacuum triode. In the OFF state, the carriers face a barrier [cf. the simplified band diagram in Fig. 1(c)]. Note that although graphene has no bandgap for lateral transport, it poses a barrier for transport in the normal direction (bandgap at Γ [13]). In the ON state, carriers tunnel through the emitter–base (E–B) insulator (EBI) and the base control electrode (graphene) into the conducting band of the base–collector (B–C) insulator [(BCI); Fig. 1(d)].

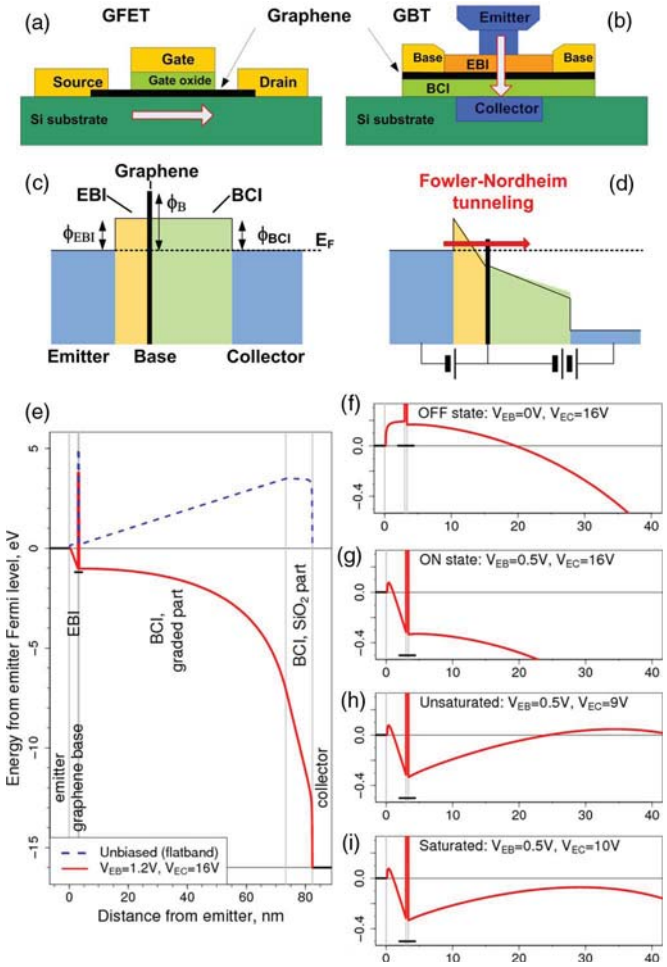

Fig. 1. (a)–(d) Schematic cross sections of (a) GFET and (b) GBT and the schematic band diagrams of (c) an unbiased and (d) biased GBT. (e)–(i) Calculated band diagrams of a high-power GBT with graded BCI. V_{EB} is given with respect to bias compensating the work function difference between graphene and emitter (flatband). (e) Potential distribution at (blue dashed) flatband and at (red solid) $V_{\text{EB}} = 1.2$ V, $V_{\text{EC}} = 16$ V. (f)–(i) Potential distribution close to graphene. At $V_{\text{EC}} = 16$ V: (f) OFF state and (g) ON state. At $V_{\text{EB}} = 0.5$ V: (h) Unsaturated regime with potential barrier in the BCI and (i) saturated regime.

There are substantial advantages when using graphene as the base material: The monatomic thickness favors ballistic transport across the base and a homogenous electric field at the base interface. Assuming that only electrons scattered within the base contribute to the base current I_B, this should reduce I_B by two orders of magnitude compared to similar HETs with a metal base. In contrast to metals, the base resistivity is not

Manuscript received February 9, 2012; accepted February 23, 2012. Date of publication April 3, 2012; date of current version April 20, 2012. The work of M. C. Lemme and M. Ostling was supported by Advanced Investigator Grant (OSIRIS, 228229) from the European Research Council. The review of this letter was arranged by Editor A. Ortiz-Conde.

W. Mehr, J. Dabrowski, J. C. Scheytt, and G. Lupina are with the IHP GmbH, 15236 Frankfurt (Oder), Germany (e-mail: mehr@ihp-microelectronics.com).

G. Lippert is with IHP GmbH, 15236 Frankfurt (Oder), Germany.

Y.-H. Xie is with the Department of Materials Science and Engineering, University of California, Los Angeles, CA 90095-1595 USA.

M. C. Lemme and M. Ostling are with the KTH Royal Institute of Technology, 10044 Stockholm, Sweden.

Color versions of one or more of the figures in this letter are available online at http://ieeexplore.ieee.org.

Digital Object Identifier 10.1109/LED.2012.2189193

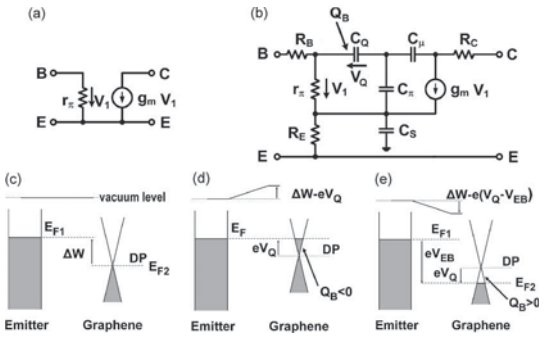

Fig. 2. (a)–(b) SS models at (a) low frequency and (b) HF. (c)–(d) Quantum capacitance: (c) Before and (d) after the equilibration of Fermi levels and (e) under bias $V_{\rm EB}$. $\Delta W \approx 0.6$ eV and $\Delta W - eV_Q \approx 0.3$ eV.

limited by pinholes; values around 100 Ω/sq are achievable [14]. Graphene is chemically inert, reducing issues with process-induced interface reactions. Although the inhomogeneity of graphene doping may lead to inhomogeneous I_C and to local heating, this may be uncritical thanks to the high thermal conductivity of graphene.

III. Device Design Aspects

GBT needs to be carefully engineered for an optimal operation. The EBI must be thin to yield high output currents. The EBI barrier $\Phi_{\rm EBI}$ is controlled by the E–B voltage $(V_{\rm EB})$ applied to the graphene. In the ON state, electrons must cross the BCI easily. However, for good power performance, the BCI should withstand $V_{\rm BC} \approx 10$ V, which implies a high tunneling barrier. The structure shown in Fig. 1(e) addresses these issues. SiO_2 is used on the collector side, and a graded silicate is used on the base side. In the graded part, the dielectric constant and the BCI barrier $(\Phi_{\rm BCI})$ vary with the distance from the base. This can be achieved with a gradually decreasing metal content across the dielectric [15]. The barrier on the collector side is controlled by the B–C voltage $V_{\rm BC}$. When $V_{\rm BC}$ is high enough, most of the electrons encounter no barrier [Fig. 1(e)]. SiO_2 thickness allows for high output voltages, i.e., for good power performance. This reveals the several advantages of the GBT compared to GFETs: 1) GBTs allow for high $I_{\rm on}/I_{\rm off}$ current ratios [Fig. 3(b) and (c)]; 2) GBTs show current saturation in the output characteristics because for high $V_{\rm EC}$, nearly all electrons travel above the BCI barrier. Thus, $I_{\rm on}$ is limited by the EBI barrier and independent of $V_{\rm EC}$ [Fig. 1(i)]; and 3) Tunneling is a fast process. Even at 2.5 THz, the current response of a tunneling diode resembles the dc curve. With the transport distance below 100 nm, delays due to diffusion should stay below a picosecond [16].

IV. SS Modeling and Comparison With HBT

A terahertz transistor may work as an HF linear small-signal (SS) amplifier. SS models with and without parasitics are shown in Fig. 2(a) and (b). The transconductance g_m becomes

$$g_m = \frac{\partial i_C}{\partial v_1} = \frac{\beta_0}{\beta_0 + 1}\frac{\partial i_E}{\partial v_1} \approx \frac{\partial i_E}{\partial v_1} \tag{1}$$

where v_1 is the SS voltage (i.e., $V_{\rm BE,ac} = V_{\rm BE,dc} + v_{1,\rm ac}$ and the amplitude of the ac signal v_1 is small), i_c and i_b are the SS collector and base currents, respectively, and $\beta_0 = i_c/i_b \gg 1$ is the SS current gain.

The HF-SS model [Fig. 2(b)] assumes metallic emitter and collector, and graphene base. R_B denotes the resistance of the base contact and of the graphene layer, R_C and R_E represent the collector and emitter resistances, r_π and r_μ are the differential resistances of EBI and BCI, and C_π and C_μ are their plate capacitances. $C_Q = |\partial Q_B/V_Q| = \kappa|V_Q|$ is the quantum capacitance of graphene $\kappa = 25$ μF/cm^2/V [17]. Q_B is the charge accumulated in graphene, and eV_Q has the physical meaning of the Fermi energy in graphene, measured with respect to the Dirac point [(DP); Fig. 2(c)–(e)]. Neglecting the substrate capacitance C_s and delays due to the diffusion of carriers, the frequency response is

$$\tau = \frac{dQ_B}{di_C} = \frac{C_{\rm TOT}}{g_m} \quad f_T = \frac{1}{2\pi\tau} = \frac{1}{2\pi}\frac{g_m}{C_{\rm TOT}} \tag{2}$$

$$C_{\rm TOT} = \frac{C_Q(C_\pi + C_\mu)}{C_Q + C_\pi + C_\mu} \tag{3}$$

$$V_Q = \frac{C_\pi + C_\mu}{s\kappa}\left(\sqrt{1 + 2\kappa\frac{|C_\pi U_{\rm EB} + C_\mu U_{\rm CB}|}{(C_\pi + C_\mu)^2}} - 1\right) \tag{4}$$

with $s = \text{sign}(C_\pi U_{\rm EB} + C_\mu U_{\rm CB})$, $U_{\rm EB} = V_{\rm EB} - \Delta W$, $U_{\rm CB} = V_{\rm CB} + \Delta W$, and $V_{\rm CB} = V_{\rm EB} - V_{\rm EC}$. The accumulated charge is $Q_B = 1/2s\,\kappa V_Q^2$. For the metallic base, one obtains $C_{\rm TOT} = C_\pi + C_\mu$[18]; V_Q is then zero.

V. Quantum-Mechanical Simulations

Graphene is semimetallic, with the DP in the corner of the 2-D first Brillouin zone (high lateral momentum). In the GBT, electrons tunnel through the EBI, and most of them are likely to enter the graphene with small lateral momentum. For such electrons, there is an energy gap in the graphene (at Γ). To verify if this makes graphene a tunneling barrier, we simulated the tunneling across the graphene placed between unbiased cobalt electrodes in vacuum. The self-consistent band structure obtained from *ab initio* atomistic calculations was used. The insertion of the graphene between the electrodes separated by 1.9 nm results in a tunneling spectrum that is roughly proportional to that obtained for 1.7-nm separation and no graphene. Thus, graphene slightly reduces the vacuum barrier strength. This is largely due to work function difference between cobalt and graphene: Graphene becomes positively charged so that the distance to vacuum energy decreases as the electron approaches the graphene sheet. A fully transparent or scattering-only sheet would reduce the vacuum thickness by about 0.35 nm (i.e., by the thickness of graphene) even without any work function difference. This does not happen; hence, graphene is a barrier, not a transparent layer.

We performed a quantum-mechanical simulation of the GBT. The tunneling parameters cannot be derived reliably from our atomistic data. For that reason, the simulation should be viewed as a zero-order estimate of a GBT in action. The Schrödinger equation with open-boundary conditions was solved numerically for one-band effective potential rounded up by image force at interfaces with emitter and collector. No self-consistent term was added as the distribution of the potential in the vicinity of graphene is not known exactly. No scattering effects were included; the temperature corresponds to the Fermi distribution of electron energies. We approximate the tunneling barrier as a rectangle with $d = 0.35$ nm and $\Phi_B = 5$ eV (the conduction band edge at Γ is between 3.7 and 7 eV [19], [20]). The effective mass was set to 0.3, a conservative value typical for, e.g.,

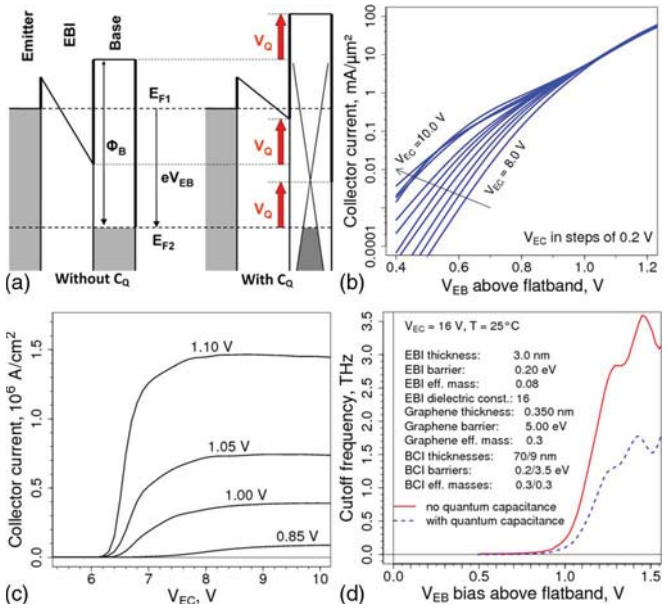

Fig. 3. (a) Effect of C_Q on the EBI electric field and on the effective Φ_B. (b) Transfer characteristics for common emitter operation. (c) Output characteristics for various V_{EB}. (d) Transition frequency f_T obtained (solid) without C_Q effects and (broken) with C_Q [cf. (2)] is plotted against $V = V_{\mathrm{EB}} - V_Q$, as this defines the EBI electric field. $V_Q \approx 0.3$ V for $V \approx 1.3$ V. Above 1.2 eV, quantum oscillations in f_T begin.

SiO_2. We performed the calculations with and without quantum capacitance effects. Quantum capacitance lowers C_{TOT}, increasing f_T. However, in a realistic device, $-C_\pi U_{\mathrm{EB}}$ will exceed $C_\mu U_{\mathrm{CB}}$; hence, $Q_B > 0$. This reduces the electric field in EBI and increases the effective Φ_B [Fig. 3(a)], decreasing g_m and, thus, also f_T. With increasing ΔW, the f_T degradation becomes less pronounced.

Fig. 3(b) and (c) shows the simulated transfer and output characteristics for operation as a power amplifier. These curves underscore the potential of the GBT, with the I_C switching over several orders of magnitude [Fig. 3(b)] and I_C saturation [Fig. 3(c)]. We estimate that for a terahertz operation [Fig. 3(d)] at $V_{\mathrm{EB}} \approx 1$ V, the EBI should not be thicker than 3–5 nm, and its energy barrier Φ_{EBI}, at no bias, should be 0.4 eV or less. In our estimations with $V_{\mathrm{EC}} = 16$ V, the electric field in SiO_2 is close to the critical field and below the critical field in the rest of the BCI. Unpinned Er_2Ge_3/Ge is assumed for the emitter/EBI. This should be viable as the interface between Ge and a germanide can be unpinned by, e.g., P [21]. The work function of Er_2Ge_3, 4.05 eV, matches the electron affinity of Ge, 4.0 eV. Assuming that the Er_2Ge_3/Ge interface can be unpinned as efficiently as for PrGe/Ge, we take $\Phi_{\mathrm{EBI}} = 0.2$ eV at no bias. For the graded part of the BCI, we use $Ti_xSi_{1-x}O_2$. The barrier at graphene/TiO_2 is assumed the same as that at Ge/graphene [22]. Fig. 3(d) compares f_T obtained without C_Q influence ($C_Q \to \infty, V_Q \to 0$) and with C_Q (using $\Delta W = 0.6$ V).

VI. Conclusion

A new device, GBT, has been proposed and analyzed. The key feature is the use of graphene as the base electrode in a HET configuration. Distinct advantages are that graphene is pinhole free and does not interact chemically with adjacent materials. Graphene is also a highly conductive one-atom thick film which does not scatter the electrons injected from the emitter to the base. Simulated GBT transfer characteristics show switching over several orders of magnitude, and output characteristics show clear saturation. We proposed and evaluated a specific material solution for GBT indicating the feasibility of a terahertz operation.

Acknowledgment

The authors would like to thank F. Driussi, P. Palestri, and L. Selmi for discussions. Atomistic calculations have been done at the Jülich Supercomputing Centre, Germany, NIC project hfo06.

References

[1] S. O. Koswatta, A. Valdes-Garcia, M. B. Steiner, Y.-M. Lin, and P. Avouris, "Ultimate RF performance potential of carbon electronics," *IEEE Trans. Microw. Theory Tech.*, vol. 59, no. 10, pp. 2739–2750, Oct. 2011.

[2] M. C. Lemme, T. J. Echtermeyer, M. Baus, and H. Kurz, "A graphene field-effect device," *IEEE Electron Device Lett.*, vol. 28, no. 4, pp. 282–284, Apr. 2007.

[3] Z. Chen, Y.-M. Lin, M. J. Rooks, and P. Avouris, "Graphene nano-ribbon electronics," *Phys. E, Low-Dimensional Syst. Nanostruct.*, vol. 40, no. 2, pp. 228–232, Dec. 2007.

[4] Y. Wu, Y.-m. Lin, A. A. Bol, K. A. Jenkins, F. Xia, D. B. Farmer, Y. Zhu, and P. Avouris, "High-frequency, scaled graphene transistors on diamond-like carbon," *Nature*, vol. 472, no. 7341, pp. 74–78, Apr. 2011.

[5] L. Liao, Y.-C. Lin, M. Bao, R. Cheng, J. Bai, Y. Liu, Y. Qu, K. L. Wang, Y. Huang, and X. Duan, "High-speed graphene transistors with a self-aligned nanowire gate," *Nature*, vol. 467, no. 7313, pp. 305–308, Sep. 2010.

[6] H. Wang, A. Hsu, J. Wu, J. Kong, and T. Palacios, "Graphene-based ambipolar RF mixers," *IEEE Electron Device Lett.*, vol. 31, no. 9, pp. 906–908, Sep. 2010.

[7] J. S. Moon, D. Curtis, D. Zehnder, S. Kim, D. K. Gaskill, G. G. Jernigan, R. L. Myers-Ward, C. R. Eddy, P. M. Campbell, K. M. Lee, and P. Asbeck, "Low-phase-noise graphene FETs in ambipolar RF applications," *IEEE Electron Device Lett.*, vol. 32, no. 3, pp. 270–272, Mar. 2011.

[8] F. Schwierz, "Graphene transistors," *Nat. Nanotechnol.*, vol. 5, no. 7, pp. 487–496, Jul. 2010.

[9] S. V. S. Rodriguez, M. Ostling, A. Rusu, E. Alarcon, and M. C. Lemme, RF performance projections of graphene FETs vs. silicon MOSFETs, arXiv:1110.0978v1, 2011.

[10] C. A. Mead, "Operation of tunnel-emission devices," *J. Appl. Phys.*, vol. 32, no. 4, pp. 646–652, Apr. 1961.

[11] M. Heiblum, "Tunneling hot electron transfer amplifiers (theta): Amplifiers operating up to the infrared," *Solid State Electron.*, vol. 24, no. 4, pp. 343–366, Apr. 1981.

[12] S. Luryi and A. Kastalsky, "Hot-electron transport in heterostructure devices," *Physica B+C*, vol. 134, no. 1–3, pp. 453–465, Nov. 1985.

[13] P. R. Wallace, "The band theory of graphite," *Phys. Rev.*, vol. 71, no. 9, pp. 622–634, May 1947.

[14] F. Bonaccorso, Z. Sun, T. Hasan, and A. C. Ferrari, "Graphene photonics and optoelectronics," *Nat. Photon.*, vol. 4, no. 9, pp. 611–622, Sep. 2010.

[15] W. Mehr and G. Lippert, "Unipolar heterojunction depletion-layer transistor," PCT/EP2009/066958, Jan. 7, 2010, Weltorganisation für Geistiges Eigentum.

[16] T. C. L. G. Sollner, P. E. Tannenwald, C. D. Parker, and D. D. Peck, "Resonant tunneling through quantum wells at frequencies up to 2.5 THz," *Appl. Phys. Lett.*, vol. 43, no. 6, pp. 588–590, Sep. 1983.

[17] H. Xu, Z. Zhang, and L.-M. Peng, "Measurements and microscopic model of quantum capacitance in graphene," *Appl. Phys. Lett.*, vol. 98, no. 13, pp. 133 122-1–133 122-3, Mar. 2011.

[18] P. R. Gray, P. J. Hurst, S. H. Lewis, and R. G. Meyer, *Analysis and Design of Analog Integrated Circuits*. Hoboken, NJ: Wiley, 2001.

[19] R. Claessen, H. Carstensen, and M. Skibowski, "Conduction-band structure of graphite single crystals studied by angle-resolved inverse photoemission and target-current spectroscopy," *Phys. Rev. B*, vol. 38, no. 17, pp. 12 582–12 588, Dec. 1988.

[20] Z. Klusek, "Investigations of splitting of the π bands in graphite by scanning tunneling spectroscopy," *Appl. Surf. Sci.*, vol. 151, no. 3/4, pp. 251–261, Oct. 1999.

[21] C. Henkel, S. Abermann, O. Bethge, G. Pozzovivo, S. Puchner, H. Hutter, and E. Bertagnolli, "Reduction of the PtGe/Ge electron Schottky-barrier height by rapid thermal diffusion of phosphorus dopants," *J. Electrochem. Soc.*, vol. 157, no. 8, pp. H815–H820, Jun. 2010.

[22] A. C. Tuan, T. C. Kaspar, T. Droubay, J. W. Rogers, and S. A. Chambers, "Band offsets for the epitaxial $TiO_2/SrTiO_3/Si(001)$ system," *Appl. Phys. Lett.*, vol. 83, no. 18, pp. 3734–3736, Nov. 2003.